Electronic Supplementary Material (ESI) for Journal of Materials Chemistry

Supporting Information

Optical and Electrical Effects of Gold Nanoparticles in the active layer of Polymer Solar Cells

Charlie C. D. Wang[a], Wallace C. H. Choy[a]*, Chunhui Duan[b], Dixon D. S. Fung[a], Wei E.I. Sha[a], Feng-xian Xie[a], Fei Huang[b]*, and Yong Cao[b]

[a]Department of Electrical and Electronic Engineering, University of Hong Kong, Pokfulam Road, Hong Kong, China.

[b]Institute of Polymer Optoelectronic Materials & Devices, State Key Laboratory of Physics and Chemistry of Luminescence, South China University of Technology, Guangzhou 510640, P. R. China

* to whom correspondence should be addressed: email: chchoy@eee.hku.hk; Tel: (852)-28578485, Fax: (852) 2559-8738; msfhuang@scut.edu.cn, Tel: (86)-20-8711-4346.

Supplementary A

Supplementary Figures

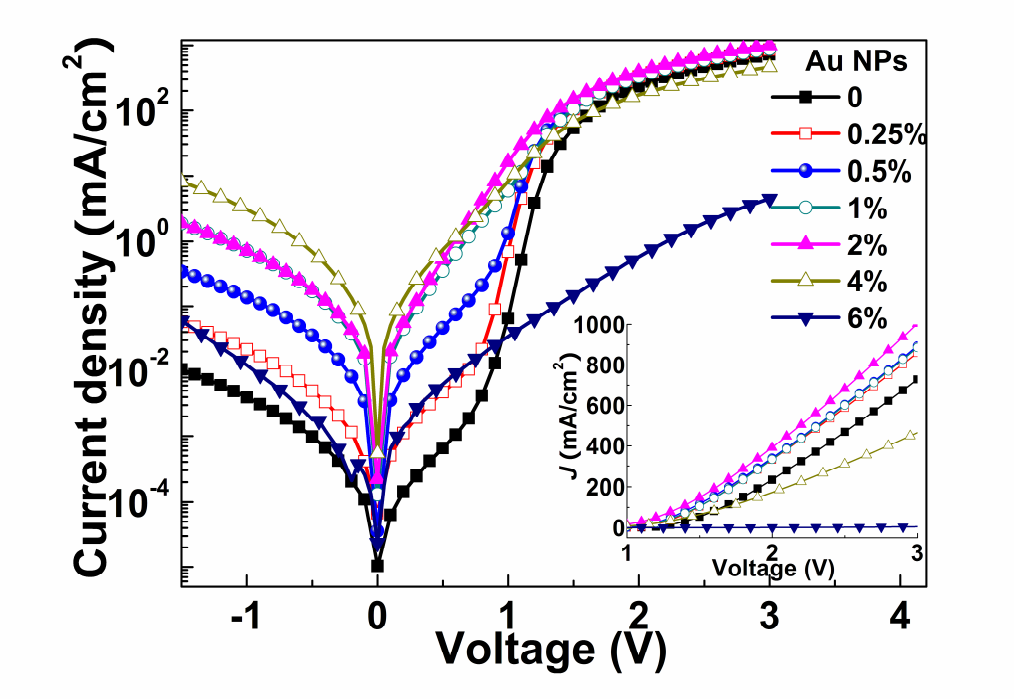

Fig. SA1 The dark current-voltage characteristics of the representative Au NP incorporated PSCs.

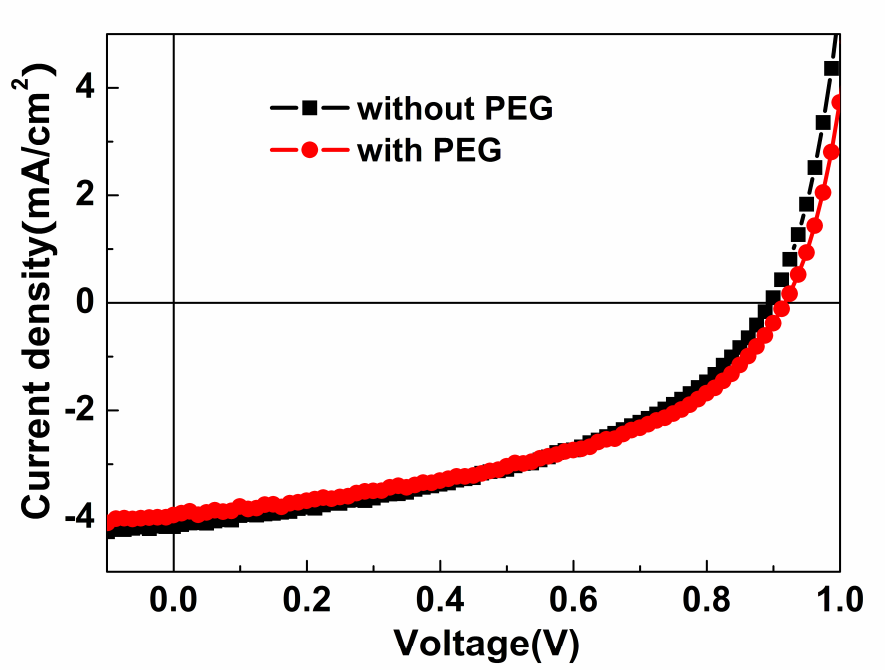

Fig. SA2 The effect of PEG on the current-voltage characteristics of PSCs.

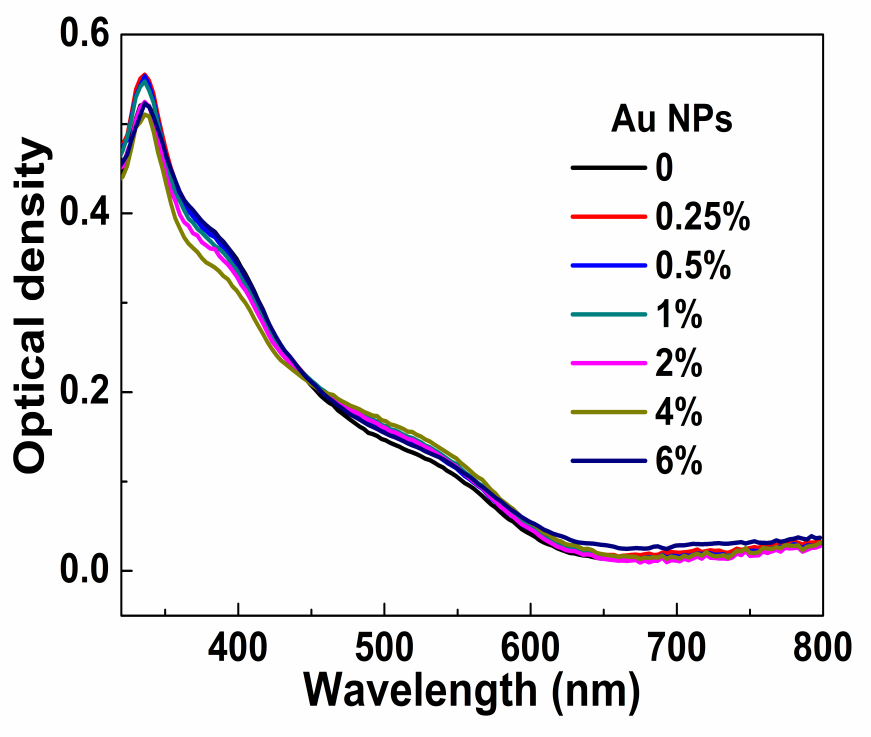

Fig. SA3 The optical densities for the PSCs incorporated with different Au NP concentrations.

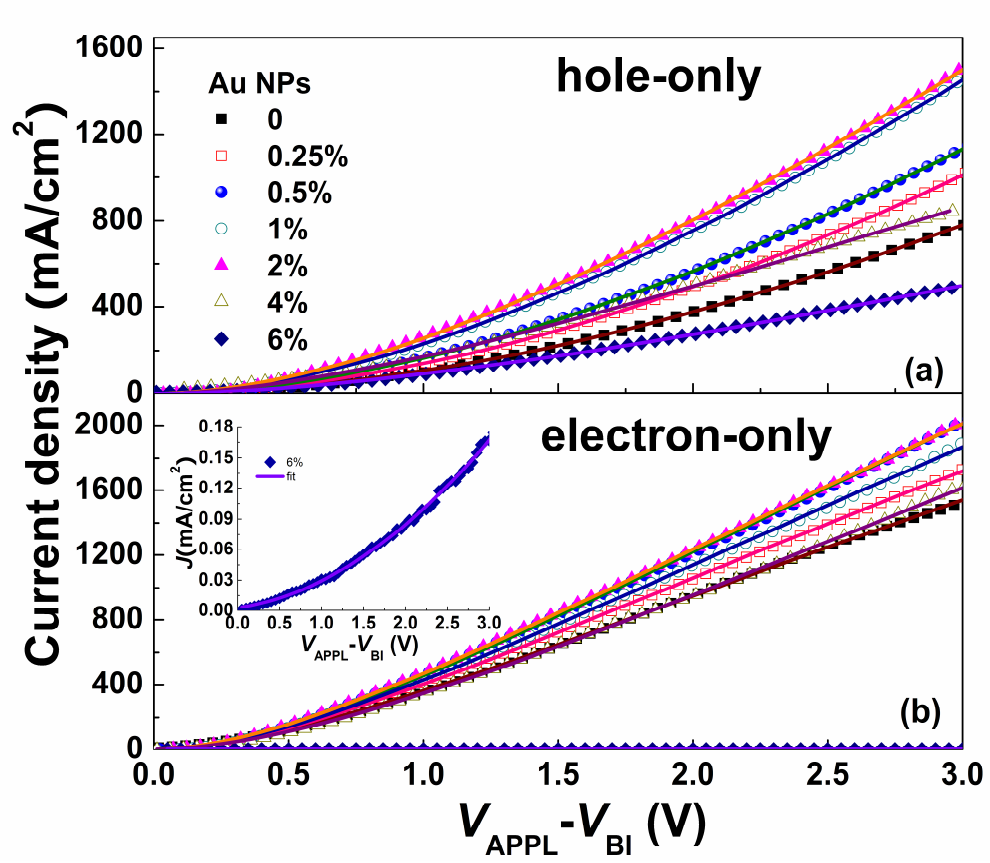

Fig. SA4 Experimental data (symbols) and fitted *J-V* curves (solid lines) of (a) hole-only devices (b) electron-only devices. The electrical conductivity of electron-only device with 6 wt% Au NP concentration is rather low and thus is shown in the inset of (b).

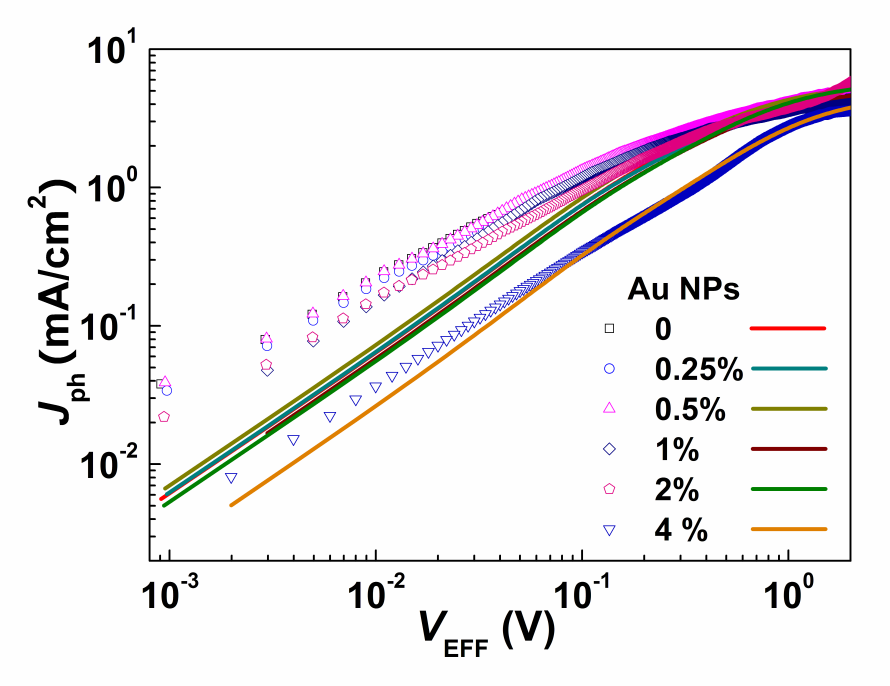

Fig. SA5 Experimental data (symbols) and fitted curves (solid lines) of photocurrent versus effective voltage for PSCs incorporated with different Au NP concentrations.

Supplementary B

In order to understand the detail physics of plasmonic effects of Au NPs on PSCs, we build an efficiency model to rigorously solve Maxwell's equations. We adopt the fast algorithm of volume integral equation - Fast Fourier transform (VIE-FFT) to solve Maxwell's equations. Details of the model are described as below.

1 Volume Integral Equation Method

The scattered electric field generated by the volumetric polarization current $\mathbf{J}$ can be written as

$$\mathbf{E}^s(\mathbf{r}) = -j_0\omega\mu_0\int_v \overline{\mathbf{G}}(\mathbf{r},\mathbf{r}')\cdot\mathbf{J}(\mathbf{r}')d\mathbf{r}' \tag{1}$$

where ω is the angular frequency, and $\overline{\mathbf{G}}(\mathbf{r},\mathbf{r}')$ is the dyadic Green's function given by

$$\overline{\mathbf{G}}(\mathbf{r},\mathbf{r}') = \left(\bar{\mathbf{I}} + \frac{\nabla\nabla}{k_0^2}\right)g(\mathbf{r},\mathbf{r}'), g(\mathbf{r},\mathbf{r}') = \frac{\exp\left(-jk_0|\mathbf{r}-\mathbf{r}'|\right)}{4\pi|\mathbf{r}-\mathbf{r}'|} \tag{2}$$

where k_0 is the wavenumber of free space. For the non-magnetic optical materials ($\mu_r = 1$), the volume integral equation (VIE) is of form

$$\mathbf{E}^i(\mathbf{r}) = \frac{\mathbf{J}(\mathbf{r})}{j_0\omega\left(\varepsilon(\mathbf{r})-\varepsilon_0\right)} - \mathbf{E}^s(\mathbf{r}) \tag{3}$$

where $\varepsilon(\mathbf{r})$ is the position-dependent permittivity of the inhomogeneous materials, and $\mathbf{E}^i(\mathbf{r})$ is the incident electric field.

Considering the Cartesian coordinate system, we use the short notation (u_1,u_2,u_3) substituting for (x,y,z), then we have

$$\begin{bmatrix} E_1^s \\ E_2^s \\ E_3^s \end{bmatrix} = \begin{bmatrix} L_{11} & L_{12} & L_{13} \\ L_{21} & L_{22} & L_{23} \\ L_{31} & L_{32} & L_{33} \end{bmatrix}\begin{bmatrix} J_1 \\ J_2 \\ J_3 \end{bmatrix} \tag{4}$$

where

$$L_{ij} = \begin{cases} L_{ii}^c + L_{ii}^q, i = j \\ L_{ij}^q, i \neq j \end{cases} \tag{5}$$

$$L_{ii}^{c} J_i = -j_0 \omega \mu_0 \int_v g(\mathbf{r}, \mathbf{r}') J_i(\mathbf{r}') d\mathbf{r}' \tag{6}$$

$$L_{ij}^{q} J_j = \frac{-j_0}{\omega \varepsilon_0} \frac{\partial}{\partial u_i} \int_v g(\mathbf{r}, \mathbf{r}') \frac{\partial J_j(\mathbf{r}')}{\partial u_j'} d\mathbf{r}' \tag{7}$$

Using the rooftop basis functions to expand the unknown currents, we have

$$\mathbf{J}(\mathbf{r}) = \sum_{i=1}^{3} \mathbf{u}_i \sum_{k,m,n} J_i^D(k,m,n) T_{k,m,n}^i \tag{8}$$

where $T_{k,m,n}^1$, $T_{k,m,n}^2$, and $T_{k,m,n}^3$ are the volumetric rooftop functions given by

$$\begin{aligned} T_{k,m,n}^1 &= \Lambda_k(u_1)\Pi_m(u_2)\Pi_n(u_3) \\ T_{k,m,n}^2 &= \Pi_k(u_1)\Lambda_m(u_2)\Pi_n(u_3) \\ T_{k,m,n}^3 &= \Pi_k(u_1)\Pi_m(u_2)\Lambda_n(u_3) \end{aligned} \tag{9}$$

The functions $\Lambda_k(u_1)$ and $\Pi_m(u_2)$ are defined by

$$\begin{aligned} \Lambda_k(u_1) &= \begin{cases} 1 - \dfrac{|u_1 - k\Delta u_1|}{\Delta u_1}, & |u_1 - k\Delta u_1| \le \Delta u_1 \\ 0, & \text{else} \end{cases} \\ \Pi_m(u_2) &= \begin{cases} 1, & \left| u_2 - \left(m - \dfrac{1}{2} \right) \Delta u_2 \right| < \dfrac{\Delta u_2}{2} \\ 0, & \text{else} \end{cases} \end{aligned} \tag{10}$$

The cuboid cells are employed to discretize the structure to be modeled. Here, Δu_1 and Δu_2 are the grid sizes of each small cuboid along x and y directions, respectively. Other functions in (9) can be defined as the same way.

As a result, the discretized form for the operator L_{ii}^{c} in (6) can be written as

$$L_{ii}^{D,c} J_i^D = -j_0 \omega \mu_0 g^D \otimes J_i^D \tag{11}$$

where $\otimes$ denotes the discrete convolution

$$g^D \otimes J_i^D = \sum_{k,m,n} g^D(k - k', m - m', n - n') J_i^D(k', m', n') \tag{12}$$

and

$$g^D(k,m,n)=\int_0^{\Delta u_1}\int_0^{\Delta u_2}\int_0^{\Delta u_3} g(u_{1,k}-u_1',u_{2,m}-u_2',u_{3,n}-u_3')du_1'du_2'du_3' \tag{13}$$

Likewise, the operator $L_{12}^{D,q}$ in (7) can be discretized as

$$\begin{aligned} L_{12}^{D,q}J_2^D &= \frac{-j_0}{\omega\varepsilon_0\Delta u_1\Delta u_2}\left[g^D(k+1,m,n)-g^D(k,m,n)\right] \\ &\otimes\left[J_2^D(k,m,n)-J_2^D(k,m-1,n)\right] \\ &= \frac{-j_0}{\omega\varepsilon_0\Delta u_1\Delta u_2}\left\{\left[g^D(k+1,m,n)-g^D(k,m,n)\right]\right. \\ &\left.-\left[g^D(k+1,m-1,n)-g^D(k,m-1,n)\right]\right\}\otimes J_2^D(k,m,n) \end{aligned} \tag{14}$$

where the finite-difference method is used for the smooth approximation of the dyadic Green's function.

The computations of the discrete convolutions can be performed efficiently by means of cyclic convolutions and fast Fourier transform (FFT), which is similar to the discrete dipole approximation (DDA) method.

2 The Biconjugate Gradient Stabilized Algorithm

The resulting VIE matrix equation can be expressed as

$$Ax=b$$

The procedure of the biconjugate gradient stabilized (BI-CGSTAB) algorithm is given as follows:

Give an initial guess x_0, we have

$$\begin{aligned} &r_0=b-Ax_0,\hat{r}_0=r_0 \\ &\rho_0=\alpha=\omega_0=1 \\ &v_0=p_0=0 \end{aligned}$$

Iterate for $i=1,2,\cdots,n$

$$\rho_i = \langle \hat{r}_0, r_{i-1} \rangle$$
$$\beta = (\rho_i / \rho_{i-1})(\alpha / \omega_{i-1})$$
$$p_i = r_{i-1} + \beta(p_{i-1} - \omega_{i-1} v_{i-1})$$
$$v_i = A p_i$$
$$\alpha = \rho_i / \langle \hat{r}_0, v_i \rangle$$
$$s = r_{i-1} - \alpha v_i$$
$$t = A s$$
$$\omega_i = \langle t, s \rangle / \langle t, t \rangle$$
$$x_i = x_{i-1} + \alpha p_i + \omega_i s$$
$$r_i = s - \omega_i t$$

Terminate when

$$\frac{\| r_i \|_2}{\| b \|_2} < \eta$$

where η is the tolerance that specifies the desired accuracy of solution.

Supplementary C

The electrical properties of PSCs have been theoretically studied by solving the organic semiconductor equations involving Poisson, drift-diffusion, and continuity equations [refer to: Mihailetchi et al. Phys. Rev. Lett. 93, 216601 (2004); Koster et al. Phys. Rev. B 72, 085205 (2005); Sievers et al. J. Appl. Phys. 100, 114509 (2006)]. The field dependent mobility uses the Frenkel-Poole form $\mu=\mu_0\exp(F/F_0)$. The Braun-Onsager model is employed for the exciton dissociation. The boundary conditions for ohmic or schottky contacts are also taken into account.

Due to the very thin active layer (~ 65 nm), it can be assumed the generation rate of bound electron-hole pairs (G_{max}) is uniform. G_{max} can be obtained from the measured absorption spectra. The electron and hole mobilities can be obtained by fitting the *J-V* curves of the measured electron- and hole-only devices following the space-charge limited current (SCLC) model. The highest occupied molecular orbital (HOMO) is -5.32 eV as measured by cyclic voltammetry (CV) method and the lowest unoccupied molecular orbital (LUMO) is -3.27 eV calculated from HOMO level and optical bandgap. The exciton decay rate (k_F) of exciton and charge separation distance (a) can be fitted to make our theoretical *J-V* curves best fit to the experimental *J-V* curves. The detailed analysis can be referred to "Results and discuss: Part 3.5" in the manuscript.

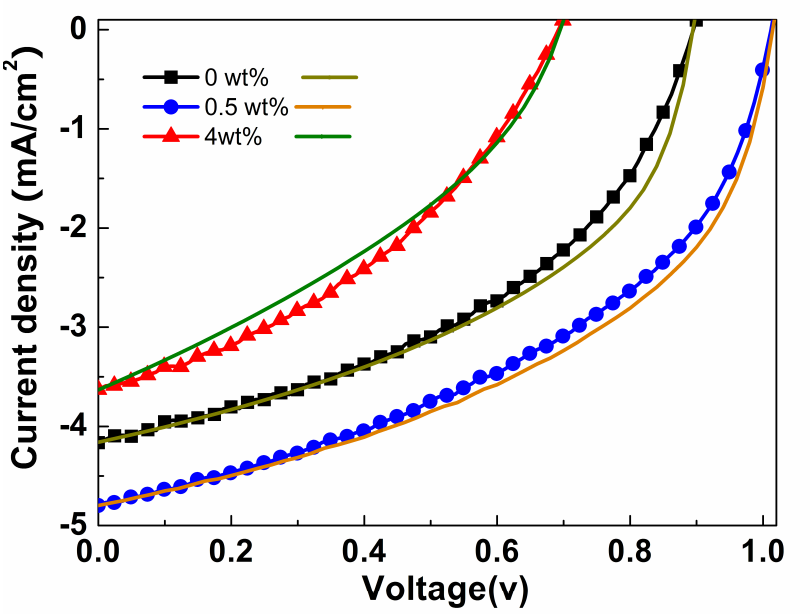

Fig. SC1 *J-V* characteristics of the PSCs with different Au NPs concentration under AM 1.5G illumination at 100 mW/cm^2. The symbols denote experimental data (squares: without Au NPs; circles: Au NPs 0.5 wt%; triangles: Au NPs 4 wt%). The solid lines denote theoretical results.